Structural basis of Flavivirus NS1 assembly and antibody recognition

Melissa A. Edeling[a], Michael S. Diamond[a,b,c], and Daved H. Fremont[a,d,1]

Departments of [a]Pathology and Immunology, [b]Medicine, [c]Molecular Microbiology, and [d]Biochemistry and Molecular Biophysics, Washington University in St. Louis, St. Louis, MO 63110

Edited* by Stephen C. Harrison, Children's Hospital, Harvard Medical School and Howard Hughes Medical Institute, Boston, MA, and approved February 7, 2014 (received for review November 25, 2013)

The Flavivirus nonstructural protein 1 (NS1) is a conserved, membrane-associated and secreted glycoprotein with replication and immune evasion functions. Secreted NS1 is a hexameric, barrel-shaped lipoprotein that can bind back to the plasma membrane of cells. Antibodies targeting cell surface-associated NS1 can be protective in vivo in a manner dependent on Fc effector functions. We describe here the crystal structure of a C-terminal fragment (residues 172–352) of West Nile (WNV) and Dengue virus NS1 proteins at 1.85 and 2.7 Å resolution, respectively. $NS1_{172–352}$ assembles as a unique rod-shaped dimer composed of a 16-stranded β-platform flanked on one face by protruding connecting loops. We also determined the 3.0 Å resolution structure of WNV $NS1_{172–352}$ with the protective 22NS1 antibody Fab, which engages the loop-face of the rod. The head-to-head $NS1_{172–352}$ dimer we observe in crystal lattices is supported by multiangle light and small-angle X-ray scattering studies. We used the available cryo-electron microscopy reconstruction to develop a pseudoatomic model of the NS1 hexamer. The model was constructed with the $NS1_{172–352}$ dimeric rod aligned with the long axis of the barrel, and with the loop-face oriented away from the core. Difference densities suggest that the N-terminal region of NS1 forms globular lobes that mediate lateral contacts between dimers in the hexamer. Our model also suggests that the N-terminal lobe forms the surface of the central cavity where lipid binding may occur.

virology | structural biology | human pathogen | immune epitope

The Flavivirus genus of the *Flaviviridae* family comprises globally important viruses [e.g., West Nile (WNV), Dengue (DENV), Japanese encephalitis (JEV), yellow fever (YFV), and tick-borne encephalitis (TBEV) viruses] that are transmitted by insects, infect almost 400 million people per year, and cause severe clinical syndromes, including hemorrhagic fever, vascular shock, liver failure, flaccid paralysis, and encephalitis (1, 2). The ∼10.7-kb positive sense RNA Flavivirus genome is translated as a single polyprotein, which is then cleaved posttranslationally into three structural proteins (C, prM/M, E) and seven nonstructural (NS) proteins (NS1, NS2A, NS2B, NS3, NS4A, NS4B, NS5) by virus- and host-encoded proteases (3). Flavivirus RNA replication occurs along the cytosolic face of the endoplasmic reticulum (ER) and requires the enzymatic actions and scaffolding functions of several NS proteins, including the viral helicase and protease (NS3), RNA-dependent RNA polymerase (NS5), and the small transmembrane proteins (NS4A and NS4B) (3).

Flavivirus NS1 is a conserved nonstructural N-linked glycoprotein (∼48 kDa) with six invariant intramolecular disulfide bonds. NS1 is synthesized as a monomer, dimerizes after posttranslational modification in the lumen of the ER, is processed in the *trans*-Golgi network, and secreted into the extracellular space as a hexameric lipoprotein particle (4). NS1 hexamers have a central lipid-rich core and are held together by weak hydrophobic interactions that dissociate into dimers in the presence of nonionic detergents (5–10). NS1 can be secreted at high levels into the extracellular environment, with accumulation of up to 50 μg/mL in the sera of some DENV-infected patients (11–13). NS1 also is expressed on the plasma membrane surface through several mechanisms. Secreted NS1 can bind to the plasma membrane of cells (14) through recognition of sulfated glycosaminoglycans (GAG) (15). Dimeric NS1 is expressed directly on the plasma membrane of infected cells (10, 16), although it lacks a canonical transmembrane domain or targeting motif for cellular membranes. The mechanism for this remains uncertain, although some fraction may be linked through an atypical glycosyl-phosphatidylinositol anchor (17, 18) or lipid rafts (19).

Intracellular expression of NS1 within the lumen of the ER also is required for viral replication and negative-strand viral RNA synthesis (20–22). Deletion of NS1 prevents replication and infection entirely, although viruses lacking NS1 can be complemented *in trans* by ectopic expression of NS1. Genetic and biochemical studies suggest that NS1 interacts with multiple host proteins and the transmembrane NS4A and NS4B viral proteins (23, 24). Such events could integrate key signals or provide necessary components (e.g., lipids) that facilitate RNA replication in the cytoplasm.

Extracellular NS1 is a target of humoral immune system recognition and control. Several groups also have generated protective antibodies against NS1, even though the protein is absent from the virion. A requirement for Fc effector function has been established for at least some protective anti-NS1 MAbs. Passive transfer of monoclonal antibodies (MAbs) against NS1 can protect mice against lethal infection by WNV, JEV, and YFV (25–27) and this requires an intact Fc moiety (28). Protective anti-NS1 MAbs recognize cell surface-associated forms of NS1 and trigger Fc-γ receptor-dependent phagocytosis and clearance of WNV-infected cells (29).

Significance

Flavivirus nonstructural protein 1 (NS1) is a versatile nonstructural glycoprotein that is expressed on the cell surface and secreted into the extracellular space, where it has immune evasion functions. To date, the structural biology of NS1 is limited, which has hampered a complete understanding of its functions. We describe the previously unidentified high-resolution structure of the C-terminal half of West Nile virus (WNV) and Dengue virus-1 ($NS1_{172–352}$) NS1 proteins and a separate structure of WNV $NS1_{172–352}$ with a protective antibody Fab. $NS1_{172–352}$ forms a head-to-head dimer and adopts a unique fold with an extended β-sheet platform and opposing loop face. These structures have allowed us to develop an architectural model for NS1 assembly and function.

Author contributions: M.A.E., M.S.D., and D.H.F. designed research; M.A.E. and D.H.F. performed research; M.A.E. contributed new reagents/analytic tools; M.A.E. and D.H.F. analyzed data; and M.A.E., M.S.D., and D.H.F. wrote the paper.

The authors declare no conflict of interest.

*This Direct Submission article had a prearranged editor.

Data deposition: The atomic coordinates and structure factors have been deposited in the Protein Data Bank, www.pdb.org (PDB ID codes 4OIE, 4OIG, and 4OII).

[1]To whom correspondence should be addressed. E-mail: fremont@wustl.edu.

This article contains supporting information online at www.pnas.org/lookup/suppl/doi:10.1073/pnas.1322036111/-/DCSupplemental.

NS1 also has immune evasive functions in the extracellular space, on the surface of cells, and possibly within cells. NS1 binds several complement proteins (C1q, C1s, and C4) (30, 31) and regulators (factor H, C4 binding protein, and clusterin) (32–35) and antagonizes their functions. NS1 also may disrupt Toll-like receptor 3 signaling (36) and innate immune system restriction of Flavivirus infection.

Despite three decades of intensive study, there is still limited structural understanding of Flavivirus NS1. Mutagenesis and biochemical studies have identified peptide sequences in the N terminus that modulate secretion and surface expression (37), cysteine residues that mediate intramolecular disulfide bonds (38, 39), and two conserved N-linked glycans (40–43). Antibody mapping studies have generated topology models suggesting proximity between different regions of the NS1 protein (25). Two low-resolution [23 Å (8) and 30 Å (7)] cryo-electron microscopy (cryo-EM) reconstructions of secreted NS1 revealed a barrel-like hexamer with dimensions of 9 nm in height and ∼10 nm in diameter, in which the three dimeric rods interacted along narrow lateral surfaces to form a wide central channel that was filled with lipid cargo.

To improve our understanding of how NS1 functions, we determined the atomic structure of the C-terminal 177 amino acids of WNV and DENV NS1, respectively. $NS1_{172–352}$ dimerizes in a head-to-head arrangement to form an ∼10-nm rod with one face composed of a 16-stranded β-platform and the other a complex arrangement of connecting loops, together representing a novel structural fold. We also determined the structure of WNV $NS1_{172–352}$ in a 2:2 complex with the Fab of a protective anti-NS1 antibody (22NS1). The structural epitope of this therapeutically protective antibody involved 16 contact residues on the loop face of $NS1_{172–352}$, which established the orientation of dimeric NS1 in the hexameric lipoprotein. Collectively, our studies define a unique protein fold and establish a model for the architectural arrangement of NS1 domains.

Results

Structure of the C-Terminal Domain of WNV and DENV NS1. We obtained crystals of oxidatively refolded WNV $NS1_{172–352}$ (described in *SI Experimental Procedures*) that diffracted X-rays to 1.85 Å resolution (Table S1). Monomeric $NS1_{172–352}$ (the first four residues of our protein are not visible in the electron density map) had dimensions of ∼5.6 nm × 3.6 nm at its widest point, with one smooth face comprising two extended β-sheets (designated sheets A and B and consisting of eight and three β-strands, respectively) and an opposing irregular face contributed by a complex arrangement of loop structure (Fig. 1*A*). The two β-sheets were composed of 11 β-strands and connected by an extensive array of turns (25 β- and 5 γ-turns), β-hairpins (5), and short helical structures. The crystal structure of $NS1_{172–352}$ revealed four disulfide bonds (C179-C223, C280-C329, C291-C312, and C313-C316). The disulfide bond arrangement of two (C179-C223, C280-C329) of these were assigned correctly by mass spectrometry analysis

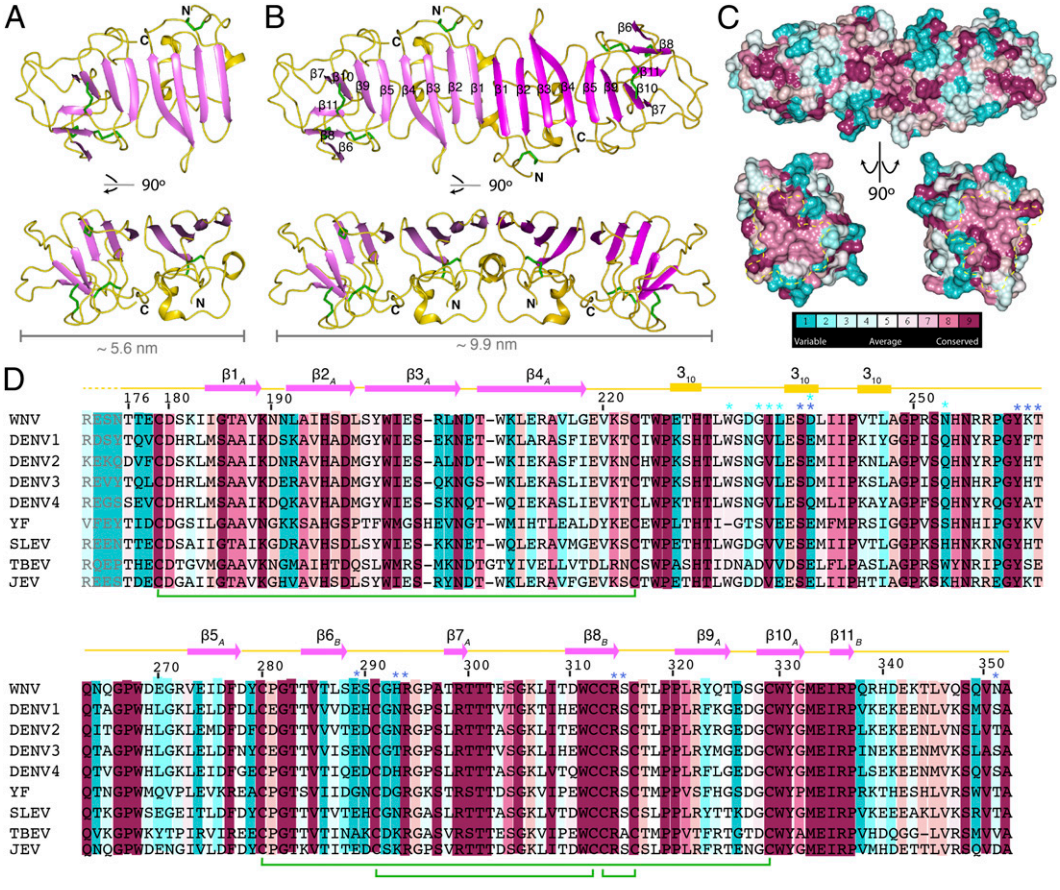

Fig. 1. Structure of WNV $NS1_{172–352}$. (*A*) Ribbon diagram of the WNV $NS1_{172–352}$ monomer. One face is created by an eight β-stranded platform flanked by a series of connecting loops and a short three β-stranded sheet. (*B*) WNV $NS1_{172–352}$ crystallizes as a head-to-head dimer that forms an extensive β-sheet platform on one face. (*C*) The dimer interface is conserved in Flavivirus NS1 homologs. The amino acid conservation among 53 NS1 homologs is mapped onto the surface of $NS1_{172–352}$ structure. Amino acid conservation is colored as in *D*. (*D*) Multiple sequence alignment compiled from 53 Flavivirus NS1 homologs (62). Representative sequences are shown. Four disulfide bonds are highlighted in green below the sequence. The two β-sheets are distinguished by the subscripts A and B. The 22NS1 epitope (Fig. 4) is marked with an asterisk (blue, contacts with heavy chain; cyan, contacts light chain).

of peptide fragments of DENV-2 NS1 (39), but disulfides involving the two adjacent cysteines (C312 and C313) were incorrectly assigned.

A comparison of the monomeric $NS1_{172–352}$ with available protein structures failed to reveal any similar overall folds. The closest structural relative with a comparatively weak DALI *z*-score of 4 (44) was the bacteriophage membrane-piercing protein (45) in which a discontinuous stretch of six β-strands aligned with the $NS1_{172–352}$ β-platform (67 residues; rmsd of 5.9 Å); like $NS1_{172–352}$, this bacteriophage protein also packs as a head-to-head dimer. We also note that the first four strands and connecting loops of $NS1_{172–352}$ (residues 176–258), that we previously described as fragment II from expression and serological analysis (25), dimerizes to form an eight β-strand platform that is remarkably similar to members of the MHC class I family of proteins, albeit with the flanking helices being replaced topologically by the extended NS1 connecting loops [DALI *z*-score of 4.2 for Research Collaboratory for Structural Bioinformatics (RCSB) 3IT8, with 103 aligned residues and rmsd of 3.9 Å] (46).

The conservation of $NS1_{172–352}$ was evaluated by analyzing the rate of evolution of individual amino acids from 53 different NS1 homologs (Fig. 1*D*), with highly conserved residues suggesting regions of structural and functional importance. $NS1_{172–352}$ had at least three conserved surface patches, with one region juxtaposed to the ends of the monomer, a second patch on the opposite face of the monomer, and a third region at one edge of the monomer (Fig. 1*C* and Fig. S1).

$NS1_{172–352}$ Forms a Head-to-Head Dimer. Soon after translation, NS1 is transported to and displayed on the plasma membrane surface as a dimer (5, 9, 10), and secreted as a trimer of dimers (7, 8). Investigation of the potential for oligomeric assembly of $NS1_{172–352}$ revealed three interfaces in the crystal lattice (Fig. S2 *A–C* and Table S2). One of these interfaces had the potential to form a quaternary structure (47) with a combined buried surface area of 1,463 $Å^2$, which is within the range of homodimeric proteins (48). This predicted dimeric assembly extends the β-sheet structure such that two monomers lie in a head-to-head arrangement (Fig. 1 *B* and *C*) with a long axis of ∼9.9 nm. All but 5 of the 22 residues in this interface are conserved in NS1 homologs (Table S3) and more than half are hydrophobic (I183, I184, G185, A187, L206, W210, L231, W232, G233, H229, K189, K182, and H254). The combination of highly conserved residues with a hydrophobic character suggests a possible dimer interface.

We also determined the structure DENV-1 $NS1_{172–352}$ to 2.7 Å (Fig. S3). DENV-1 $NS1_{172–352}$ (the first six residues are not visible in the electron density map) crystallized with four copies in the asymmetric unit forming two head-to-head dimers remarkably similar to that observed for WNV $NS1_{172–352}$ (Fig. S2*D*). A comparison of the two dimers in the asymmetric unit of the crystal did not reveal major structural differences (rmsd of 0.50 Å for 350 α-carbons). Dimeric DENV-1 $NS1_{172–352}$ was similar to dimeric WNV $NS1_{172–352}$ (rmsd of 0.98 Å for 347 α-carbons). Thus, the overall structure of the C-terminal half of DENV-1 and WNV were similar, consistent with the level of sequence identity (57%).

To evaluate our structural prediction that $NS1_{172–352}$ forms a dimer in solution, we examined the oligomeric state of WNV $NS1_{172–352}$ by size-exclusion chromatography multiangle light scattering (SEC-MALS). The molecular weight of wild-type WNV $NS1_{172–352}$ was determined as 48.9 kDa (Fig. S4*A*) and that of an engineered double mutant, $NS1_{172–352}$ I184M + L241M, which was used for phasing by single-wavelength anomalous diffraction, was 44.5 kDa (Fig. S4*B*); both weights are approximately double that of the 21-kDa monomer. Thus, MALS analysis of WNV $NS1_{172–352}$ corroborated our structural data and revealed a dimer in solution. This finding also was confirmed for DENV $NS1_{172–352}$ (MALS molecular weight of 39 kDa) (Fig. S4*C*).

Low-Resolution Molecular Envelope of the $NS1_{172–352}$ Dimer. To assess the oligomeric assembly of $NS1_{172–352}$ in solution, we collected small-angle X-ray scattering (SAXS) data. This technique can be used to evaluate the oligomeric state and define the maximum diameter of particles in solution (49). The SAXS profile of WNV $NS1_{172–352}$ was compared with the predicted scattering of the crystal structure of monomeric and dimeric NS1 (Fig. 2*A*). A dimer of $NS1_{172–352}$ fit the experimental scattering curve well with χ^2 = 1.7 compared with the poor fit (χ^2 = 7.3) for a monomer of $NS1_{172–352}$. The maximum diameter of $NS1_{172–352}$, D_{max}, as determined by Fourier transform of the scattering data, was 9.03 nm (Fig. 2*B*). This dimension is similar to the long axis of the crystallographic $NS1_{172–352}$ dimer (9.9 nm). Ten independently generated ab initio low-resolution solution structures were averaged and the resulting molecular envelope (which agreed with the experimental scattering curve, χ^2 = 1.6) (Fig. 2*C*) compared favorably to the crystal structure dimer (Fig. 2*D*).

Pseudoatomic Model of Dimeric $NS1_{172–352}$ in Hexameric NS1. The cryo-EM reconstruction of hexameric NS1 has a long axis of ∼10 nm, which is similar to the long axis of dimeric $NS1_{172–352}$ in solution (Fig. 2*B*). We hypothesized that $NS1_{172–352}$ contains the dominant dimerization domain within hexameric NS1 and tested this by examining the fit of dimeric $NS1_{172–352}$ in the reconstruction of DENV-1 NS1 (7). We docked dimeric WNV $NS1_{172–352}$ so that it was coincident with the long axis of D3 symmetric NS1 (7), and evaluated the accuracy of the fit in Chimera (50). This analysis produced a fit such that the β-platform projected to the interior and the loop-face projected to the outside of the barrel, with a correlation coefficient of 0.956 for 3,093 of 3,122 atoms (Fig. 3*A*). However, an alternative fit (correlation coefficient of 0.952) oriented dimeric $NS1_{172–352}$ by 180° such that the β-platform faced outside of the hexameric barrel (Fig. 3*B*). We failed to achieve reasonable fits of either monomeric or dimeric $NS1_{172–352}$ into the DENV-2 NS1 hexamer cryo-EM model that had been generated using C3 symmetry, which by definition lacks a twofold axis of symmetry that is inherent in our dimer (8).

WNV $NS1_{172–352}$ Complexed with the 22NS1 Fab. We next determined the structure of WNV $NS1_{172–352}$ in complex with Fab fragments

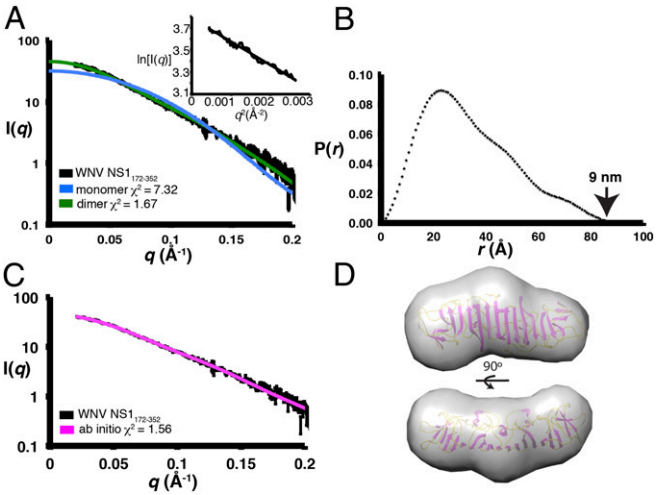

Fig. 2. $NS1_{172–352}$ is a dimer in solution. (*A*) SAXS of WNV $NS1_{172–352}$ in solution is consistent with the crystal structure of a dimer (χ^2 = 1.7) but not a monomer (χ^2 = 7.3). (*B*) The P(r) function reveals the long axis of the solution structure of WNV $NS1_{172–352}$. (*C*) The ab initio model, calculated from 10 models and averaged, fits well to the experimental scattering curve of WNV $NS1_{172–352}$ (χ^2 = 1.56). (*D*) WNV $NS1_{172–352}$ crystal structure dimer in ribbon representation docked into the averaged structural envelope (gray).

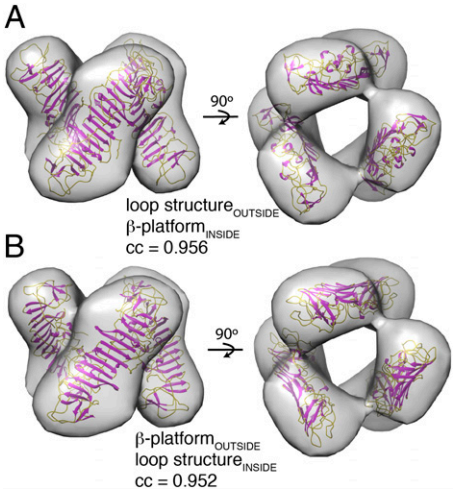

Fig. 3. Pseudoatomic model of dimeric NS1$_{172–352}$ fit into the cryo-EM reconstruction of hexameric NS1. The orientation of the (*A*) loop face projecting outside and the β-platform facing inside or (*B*) the β-platform outside and the loop face projecting inside the hexameric barrel. A quantitative measure of each fit did not distinguish between the two orientations.

of 22NS1, a therapeutically protective MAb raised against soluble hexameric NS1 that recognizes the membrane-associated protein (the first four residues are not visible in the electron density map) (25, 29). In addition to defining the epitope and providing independent evidence for an extended β-sheet dimer (Fig. S2*D*), this structure allowed us to build unambiguously a pseudoatomic resolution model of hexameric NS1 using the existing D3 cryo-EM reconstruction (7). The 22NS1 epitope mapped to the loop face of WNV NS1 NS1$_{172–352}$ (Figs. 1*D*, asterisks, and 4*A*). The combined surface area buried in the WNV NS1$_{172–352}$-22NS1 Fab complex was 2,209 Å^2, with a predominant contribution from the heavy chain (1,243 Å^2 vs. 966 Å^2 from the light chain) (Fig. 4 *C* and *D*). The interface was characterized by 27 van der Waals interactions, 8 hydrogen bonds, and 7 electrostatic interactions (Table S4) and involves 16 residues in NS1$_{172–352}$ located in the connecting loops between strands β4 and β5, β6 and β7, and β8 and β9 (Fig. 4*B*). Only 6 of the 16 contact residues of the Fab are conserved (I236, L237, S239, Y260, R294, and R314), which likely explains why 22NS1 binds to NS1 of other WNV strains but not to other JEV serocomplex family members.

We used the molecular details of the 22NS1 epitope from the crystal structure of the NS1$_{172–352}$-22NS1 Fab complex to resolve the ambiguity of the orientation of the NS1$_{172–352}$ dimer in the hexamer. Because 22NS1 MAb was raised against and recognizes soluble NS1 hexamer (25, 51), the epitope containing residues on the loop face of NS1$_{172–352}$ must be accessible for MAb binding. To achieve this result, dimeric NS1$_{172–352}$ must be positioned such that the loop-face projects outward from the hexameric barrel (Fig. 4 *C* and *D*). Difference maps using oriented NS1$_{172–352}$ reveal significant density that we interpret as the N-terminal half of NS1 (NS1$_{1–171}$) splaying at the two corners of each rod (Fig. 4*D*, *Upper Left* and *Lower Right*). This model is consistent with other antibody mapping data that identified epitopes requiring different NS1 fragments to be in close physical proximity (4, 25). We also note that the conserved glycosylation site at Asn-207 (located in the β3-β4 loop) projects toward solvent between the two N-terminal lobes (Fig. 4 *C* and *D*). Our modeling also suggests that the β-platform of dimeric NS1$_{172–352}$ projects toward the core of the barrel, where it packs against the N-terminal lobes using two highly conserved hydrophobic patches that may contribute to domain assembly (Fig. S5). The N-terminal lobes appear essential for mediating the lateral contacts of dimers in the hexameric assembly, and also serve to create the internal core of the barrel where lipids are thought to associate (7).

Discussion

Flavivirus NS1 is a multifunctional nonstructural glycoprotein that is essential for viral replication and immune evasion. NS1 is targeted by the humoral immune response and anti-NS1 antibodies can protect against Flavivirus infection in several different animal models. Despite the abundant data on different biological functions of NS1, structural insight has been limited. In this

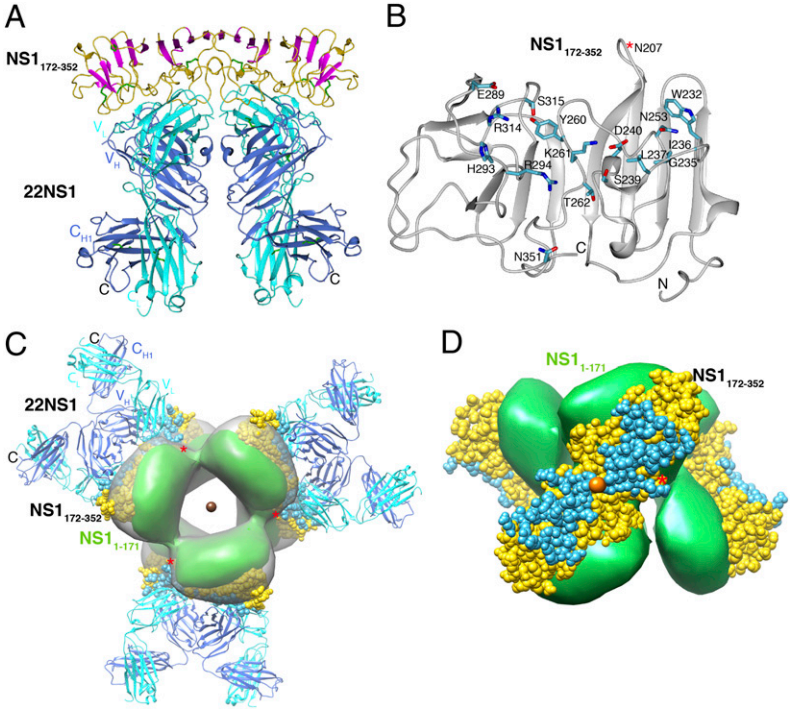

Fig. 4. Structure of WNV NS1$_{172–352}$ in complex 22NS1 Fab. (*A*) The 22NS1 Fab epitope on WNV NS1$_{172–352}$ includes 16 residues exclusively from the extensive loop face of WNV NS1$_{172–352}$. WNV NS1$_{172–352}$ is shown in magenta and gold, 22NS1 heavy chain in blue, and light chain in cyan. (*B*) WNV NS1$_{172–352}$ residues making direct contact with 22NS1 (Table S4) are shown as blue-green cylinders; NS1$_{172–352}$ is represented by gray ribbons. View is rotated 90° relative to *A*. A conserved N-linked glycan at N207 is in an exposed loop between β3 and β4 and highlighted with a red asterisk. (*C*) Pseudoatomic model of hexameric NS1 in complex with 22NS1 Fab. NS1$_{172–352}$ is represented by CPK structure in gold and the 22NS1 epitope is colored blue-green. Difference density map showing the likely position of NS1$_{1–171}$ (green surface) in NS1 hexamer, calculated by subtracting the predicted map of the fit of the trimer of NS1$_{172–352}$ dimers (after a translation of 3 Å and rotation of 12° relative to Fig. 3*A* to approach the envelope limit) from the cryo-EM reconstruction of NS1 hexamer with D3 symmetry (gray surface; contoured at 0.9 σ). A brown circle shows the view down the threefold axis of the hexamer. (*D*) The pseudoatomic model of NS1 hexamer viewed down the twofold axis shown by the orange circle. NS1$_{1–171}$ (green envelope) and NS1$_{172–352}$ (CPK structure) are represented as in *C*.

report, we determined the crystal structure of the C-terminal half of WNV and DENV-1 NS1 proteins at 1.85 and 2.7 Å resolution, respectively. $NS1_{172–352}$ assembles as a dimeric β-platform rod that we observed in three independent crystal lattices and corroborated in solution using SEC-MALS and SAXS. We also determined the crystal structure of WNV $NS1_{172–352}$ in complex with 22NS1 Fab, enabling the pseudoatomic modeling of the available cryo-EM reconstruction using D3 symmetry (7, 8). Our model positions the $NS1_{172–352}$ dimeric rod along the long axis of the hexameric barrel, with the loop face projecting outward. Six lobes of density we interpret as $NS1_{1–171}$ can be seen to splay laterally from the rods, and appear to create both the internal cavity of the barrel and the lateral contacts between dimers. This hexameric model of NS1 is consistent with a previously published scheme based on antibody epitope mapping, where the N-terminal NS1 fragment (residues 1–157) was positioned laterally to the two C-terminal NS1 fragments (residues 152–235 and 236–352, respectively) so that some MAbs (10NS1 and 17NS1) could bind epitopes that overlapped distinct NS1 fragments (25).

In the ER, Flavivirus NS1 dimerizes soon after protein synthesis (9) and these forms are expressed on the cell surface directly in infected cells without an apparent targeting motif (4, 10, 16). In comparison, the secreted form of NS1 is a hexamer and oligomerizes in the ER or early *trans*-Golgi network. Our analysis revealed that the C-terminal 177 amino acids of Flavivirus NS1 are sufficient to form a head-to-head dimer in the crystal lattice and in solution. The dimer interface is composed of conserved, mostly hydrophobic residues from both the extended β-sheet platform and the loop face of $NS1_{172–352}$. Insertion of a 56 amino influenza T-cell epitope into YFV NS1 at residue 236 resulted in loss of NS1 dimers, which is consistent with this region being critical for the dimer interface (52). A P250L mutation in WNV-Kunjin NS1 caused a loss of dimerization and was associated with defects in virus replication (53). The P250 residue, which is conserved among Flavivirus NS1, although not present at the dimer interface, is juxtaposed to it, forming hydrophobic contacts in a pocket that is lined by conserved hydrophobic amino acids (W225, H195, and I202) (Fig. 1*D*). The substitution of proline with a leucine at this position may alter this hydrophobic core and destabilize the dimeric form of the protein.

We observed the binding of several sulfate ions in the crystal structure of DENV-1 $NS1_{172–352}$, likely because of crystallization conditions. Several sulfates cluster at the dimer interface on the loop face of $NS1_{172–352}$, suggesting an extended region on the surface of NS1 for binding ligands of anionic character, possibly sulfated GAGs (54), sialic acids (55), or phospholipids (56). Indeed, DENV NS1 binds to the cell surface via interactions with sulfated GAGs (15) and hexameric NS1 is associated with lipids (7, 8).

Anti-NS1 antibodies can protect animals against Flavivirus infection. For DENV, there has been interest in this observation because immunization with NS1 might avoid enhancement of infection associated with antibodies against the envelope proteins. Establishing the epitope-specific correlates of protection is important, however, as some anti-NS1 antibodies purportedly react with host proteins and could contribute to DENV pathogenesis (57–60). Protection afforded by some anti-WNV NS1 MAbs is mediated by antibody binding to cell surface-associated NS1 and involves Fc-γ receptor-dependent phagocytosis and clearance of infected cells (29). Antibodies that fail to recognize cell-surface–bound NS1 map to the N-terminal half of NS1, suggesting that their epitopes are occluded when soluble NS1 engages the cell surface (29). A therapeutic anti-WNV MAb, 22NS1, binds the soluble hexamer and cell-associated dimer forms of NS1 (29). Its epitope, as defined by the $NS1_{172–352}$-22NS1 Fab crystal structure, is on the loop face of $NS1_{172–352}$ and is presumably solvent-exposed when NS1 is cell-associated. Comprehensive mapping of additional anti-NS1 antibodies will be necessary to distinguish epitopes with protective or pathogenic potential.

In summary, our study describes the atomic structure of NS1 by itself or in complex with Fab fragments of a protective antibody. This work establishes a model for the arrangement and function of different domains of NS1, and provides a structural template for future mutagenesis studies that define the key determinants by which NS1 interacts with host and viral factors to mediate its diverse functions.

Experimental Procedures

WNV and DENV-1 NS1 Expression, Purification, and Crystallization. WNV and DENV-1 NS1 C-terminal constructs (residues 172–352) were cloned into the NheI and NotI restriction sites of pET21a for expression in BL21 (DE3) codon plus *Escherichia coli* cells by autoinduction (61). The protein was refolded from inclusion bodies, purified by SEC and ion-exchange chromatography, concentrated to ∼8 mg/mL (WNV $NS1_{172–352}$) or 12 mg/mL (DENV-1 $NS1_{172–352}$), and crystallized by hanging-drop vapor diffusion in 20% PEG 2K MME, 0.1 M sodium acetate pH 5.4 (WNV $NS1_{172–352}$) or 20% (wt/vol) PEG 4K, 0.2 M magnesium sulfate and 10% glycerol (DENV-1 $NS1_{172–352}$). The structure of WNV $NS1_{172–352}$ was determined by single-wavelength anomalous dispersion using a mutant engineered to express two additional methionines (I184M + L241M). DENV-1 $NS1_{172–352}$ was solved by molecular replacement using WNV NS1 as a model.

Structure Determination of 22NS1 Fab-WNV NS1. Purified WNV $NS1_{172–352}$ was complexed with 22NS1 Fab (prepared by papain digestion of 22NS1 MAb) after SEC and concentrated to ∼9 mg/mL for crystallization in 8% PEG 8K and 0.1 M sodium citrate. The structure of the complex was determined by molecular replacement.

Solution Studies. The oligomeric state of WNV and DENV-1 $NS1_{172–352}$ in solution was determined by SEC-MALS using 3–8 mg/mL of purified protein. SAXS data were collected at the Advanced Light Source SIBYLS beamline 12.3.1 at three different protein concentrations (1–7.4 mg/mL) and data quality assessment and processing was performed using the ATSAS package of programs.

Docking onto the Cryo-EM Structure. Fitting of dimeric $NS1_{172–352}$ into the cryo-EM single particle analysis structures of DENV-1 NS1 (D3 symmetry, 30 Å resolution) and DENV-2 NS1 C3 symmetry, 23 Å resolution) was completed using the tool *Fit in map* in Chimera (50). The results were assessed by the corresponding correlation coefficient, which gives a quantitative measure of the fit. Dimeric $NS1_{172–352}$ produced a good fit with DENV-1 (correlation coefficient of 0.95, average map value 4.3, 19 of 3,122 atoms outside of the map contour) (7) but a poor fit to the DENV-2 (correlation coefficient of 0.62, average map value 1.5 and 1,168 of 3,122 atoms outside of the map contour) NS1 structure (8).

Structure Accession Numbers. The atomic coordinates and structure factors of WNV $NS1_{172–352}$ (CSGID target number IDP93954), DENV-1 $NS1_{172–352}$ (CSGID target number IDP00269), and 22NS1 Fab bound to WNV $NS1_{172–352}$ have been deposited in the Protein Data Bank under PDB accession nos. 4OIE, 4OIG, and 4OII, respectively.

ACKNOWLEDGMENTS. We thank Y. Levina for help with crystal preparation; J. Nix at the Advanced Light Source beamline 4.2.2 (Lawrence Berkeley Laboratories) for help with X-ray data collection; L. Huang for the 22NS1 MAb sequence; M. Flamand and F. Rey for nonstructural protein 1 (NS1) cryo-electron microscopy reconstruction data; A. Barrow, N. Tolia, R. Kuhn, and J. Smith for discussions; and G. Hura and K. Dyer and the Structurally Integrated Biology for Life Sciences Team for small-angle X-ray scattering data collection. The small-angle X-ray scattering was funded by US Department of Energy Contract DE-AC02-05CH11231. This work was supported by the Pediatric Dengue Vaccine Initiative and National Institute of Allergy and Infectious Diseases Contracts HHSN272200700058C and HHSN272201200026C (Center for Structural Genomics of Infectious Disease).

1. Bhatt S, et al. (2013) The global distribution and burden of Dengue. *Nature* 496(7446): 504–507.
2. Mackenzie JS, Gubler DJ, Petersen LR (2004) Emerging Flaviviruses: The spread and resurgence of Japanese encephalitis, West Nile and Dengue viruses. *Nat Med* 10(12, Suppl):S98–S109.
3. Lindenbach BD, Rice CM (2003) Molecular biology of Flaviviruses. *Adv Virus Res* 59: 23–61.
4. Muller DA, Young PR (2013) The Flavivirus NS1 protein: Molecular and structural biology, immunology, role in pathogenesis and application as a diagnostic biomarker. *Antiviral Res* 98(2):192–208.

5. Crooks AJ, Lee JM, Easterbrook LM, Timofeev AV, Stephenson JR (1994) The NS1 protein of tick-borne encephalitis virus forms multimeric species upon secretion from the host cell. *J Gen Virol* 75(Pt 12):3453–3460.
6. Flamand M, et al. (1999) Dengue virus type 1 nonstructural glycoprotein NS1 is secreted from mammalian cells as a soluble hexamer in a glycosylation-dependent fashion. *J Virol* 73(7):6104–6110.
7. Gutsche I, et al. (2011) Secreted Dengue virus nonstructural protein NS1 is an atypical barrel-shaped high-density lipoprotein. *Proc Natl Acad Sci USA* 108(19):8003–8008.
8. Muller DA, et al. (2012) Structure of the Dengue virus glycoprotein NS1 by electron microscopy and single particle analysis. *J Gen Virol* 93(Pt 4):771–779.
9. Winkler G, Randolph VB, Cleaves GR, Ryan TE, Stollar V (1988) Evidence that the mature form of the Flavivirus nonstructural protein NS1 is a dimer. *Virology* 162(1): 187–196.
10. Winkler G, Maxwell SE, Ruemmler C, Stollar V (1989) Newly synthesized dengue-2 virus nonstructural protein NS1 is a soluble protein but becomes partially hydrophobic and membrane-associated after dimerization. *Virology* 171(1):302–305.
11. Alcon S, et al. (2002) Enzyme-linked immunosorbent assay specific to Dengue virus type 1 nonstructural protein NS1 reveals circulation of the antigen in the blood during the acute phase of disease in patients experiencing primary or secondary infections. *J Clin Microbiol* 40(2):376–381.
12. Libraty DH, et al. (2002) High circulating levels of the Dengue virus nonstructural protein NS1 early in dengue illness correlate with the development of dengue hemorrhagic fever. *J Infect Dis* 186(8):1165–1168.
13. Young PR, Hilditch PA, Bletchly C, Halloran W (2000) An antigen capture enzyme-linked immunosorbent assay reveals high levels of the Dengue virus protein NS1 in the sera of infected patients. *J Clin Microbiol* 38(3):1053–1057.
14. Alcon-LePoder S, et al. (2005) The secreted form of dengue virus nonstructural protein NS1 is endocytosed by hepatocytes and accumulates in late endosomes: Implications for viral infectivity. *J Virol* 79(17):11403–11411.
15. Avirutnan P, et al. (2007) Secreted NS1 of Dengue virus attaches to the surface of cells via interactions with heparan sulfate and chondroitin sulfate E. *PLoS Pathog* 3(11):e183.
16. Pryor MJ, Wright PJ (1993) The effects of site-directed mutagenesis on the dimerization and secretion of the NS1 protein specified by Dengue virus. *Virology* 194(2):769–780.
17. Jacobs M, Levin M (2002) An improved endothelial barrier model to investigate Dengue haemorrhagic fever. *J Virol Methods* 104(2):173–185.
18. Noisakran S, et al. (2007) Characterization of Dengue virus NS1 stably expressed in 293T cell lines. *J Virol Methods* 142(1–2):67–80.
19. Noisakran S, et al. (2008) Association of Dengue virus NS1 protein with lipid rafts. *J Gen Virol* 89(Pt 10):2492–2500.
20. Khromykh AA, Sedlak PL, Westaway EG (1999) *Trans*-complementation analysis of the Flavivirus Kunjin ns5 gene reveals an essential role for translation of its N-terminal half in RNA replication. *J Virol* 73(11):9247–9255.
21. Lindenbach BD, Rice CM (1997) Trans-complementation of yellow fever virus NS1 reveals a role in early RNA replication. *J Virol* 71(12):9608–9617.
22. Mackenzie JM, Jones MK, Young PR (1996) Immunolocalization of the dengue virus nonstructural glycoprotein NS1 suggests a role in viral RNA replication. *Virology* 220(1):232–240.
23. Lindenbach BD, Rice CM (1999) Genetic interaction of Flavivirus nonstructural proteins NS1 and NS4A as a determinant of replicase function. *J Virol* 73(6):4611–4621.
24. Youn S, et al. (2012) Evidence for a genetic and physical interaction between nonstructural proteins NS1 and NS4B that modulates replication of West Nile virus. *J Virol* 86(13):7360–7371.
25. Chung KM, et al. (2006) Antibodies against West Nile Virus nonstructural protein NS1 prevent lethal infection through Fc gamma receptor-dependent and -independent mechanisms. *J Virol* 80(3):1340–1351.
26. Lee TH, et al. (2012) A cross-protective mAb recognizes a novel epitope within the Flavivirus NS1 protein. *J Gen Virol* 93(Pt 1):20–26.
27. Schlesinger JJ, Brandriss MW, Walsh EE (1985) Protection against 17D yellow fever encephalitis in mice by passive transfer of monoclonal antibodies to the nonstructural glycoprotein gp48 and by active immunization with gp48. *J Immunol* 135(4):2805–2809.
28. Schlesinger JJ, Foltzer M, Chapman S (1993) The Fc portion of antibody to yellow fever virus NS1 is a determinant of protection against YF encephalitis in mice. *Virology* 192(1):132–141.
29. Chung KM, Thompson BS, Fremont DH, Diamond MS (2007) Antibody recognition of cell surface-associated NS1 triggers Fc-gamma receptor-mediated phagocytosis and clearance of West Nile Virus-infected cells. *J Virol* 81(17):9551–9555.
30. Avirutnan P, et al. (2010) Antagonism of the complement component C4 by Flavivirus nonstructural protein NS1. *J Exp Med* 207(4):793–806.
31. Silva EM, Conde JN, Allonso D, Nogueira ML, Mohana-Borges R (2013) Mapping the interactions of Dengue virus NS1 protein with human liver proteins using a yeast two-hybrid system: Identification of C1q as an interacting partner. *PLoS ONE* 8(3):e57514.
32. Avirutnan P, et al. (2011) Binding of Flavivirus nonstructural protein NS1 to C4b binding protein modulates complement activation. *J Immunol* 187(1):424–433.
33. Chung KM, et al. (2006) West Nile virus nonstructural protein NS1 inhibits complement activation by binding the regulatory protein factor H. *Proc Natl Acad Sci USA* 103(50):19111–19116.
34. Krishna VD, Rangappa M, Satchidanandam V (2009) Virus-specific cytolytic antibodies to nonstructural protein 1 of Japanese encephalitis virus effect reduction of virus output from infected cells. *J Virol* 83(10):4766–4777.
35. Kurosu T, Chaichana P, Yamate M, Anantapreecha S, Ikuta K (2007) Secreted complement regulatory protein clusterin interacts with Dengue virus nonstructural protein 1. *Biochem Biophys Res Commun* 362(4):1051–1056.
36. Wilson JR, de Sessions PF, Leon MA, Scholle F (2008) West Nile virus nonstructural protein 1 inhibits TLR3 signal transduction. *J Virol* 82(17):8262–8271.
37. Youn S, Cho H, Fremont DH, Diamond MS (2010) A short N-terminal peptide motif on Flavivirus nonstructural protein NS1 modulates cellular targeting and immune recognition. *J Virol* 84(18):9516–9532.
38. Blitvich BJ, et al. (2001) Determination of the intramolecular disulfide bond arrangement and biochemical identification of the glycosylation sites of the nonstructural protein NS1 of Murray Valley encephalitis virus. *J Gen Virol* 82(Pt 9): 2251–2256.
39. Wallis TP, Huang C-Y, Nimkar SB, Young PR, Gorman JJ (2004) Determination of the disulfide bond arrangement of Dengue virus NS1 protein. *J Biol Chem* 279(20): 20729–20741.
40. Crabtree MB, Kinney RM, Miller BR (2005) Deglycosylation of the NS1 protein of Dengue 2 virus, strain 16681: Construction and characterization of mutant viruses. *Arch Virol* 150(4):771–786.
41. Muylaert IR, Chambers TJ, Galler R, Rice CM (1996) Mutagenesis of the N-linked glycosylation sites of the yellow fever virus NS1 protein: Effects on virus replication and mouse neurovirulence. *Virology* 222(1):159–168.
42. Pryor MJ, Wright PJ (1994) Glycosylation mutants of Dengue virus NS1 protein. *J Gen Virol* 75(Pt 5):1183–1187.
43. Somnuke P, Hauhart RE, Atkinson JP, Diamond MS, Avirutnan P (2011) N-linked glycosylation of Dengue virus NS1 protein modulates secretion, cell-surface expression, hexamer stability, and interactions with human complement. *Virology* 413(2): 253–264.
44. Holm L, Rosenström P (2010) Dali server: Conservation mapping in 3D. *Nucleic Acids Res* 38(Web Server issue):W545–W549.
45. Browning C, Shneider MM, Bowman VD, Schwarzer D, Leiman PG (2012) Phage pierces the host cell membrane with the iron-loaded spike. *Structure* 20(2):326–339.
46. Yang Z, West AP, Jr., Bjorkman PJ (2009) Crystal structure of TNFalpha complexed with a poxvirus MHC-related TNF binding protein. *Nat Struct Mol Biol* 16(11):1189–1191.
47. Krissinel E, Henrick K (2007) Inference of macromolecular assemblies from crystalline state. *J Mol Biol* 372(3):774–797.
48. Bahadur RP, Chakrabarti P, Rodier F, Janin J (2003) Dissecting subunit interfaces in homodimeric proteins. *Proteins* 53(3):708–719.
49. Putnam CD, Hammel M, Hura GL, Tainer JA (2007) X-ray solution scattering (SAXS) combined with crystallography and computation: Defining accurate macromolecular structures, conformations and assemblies in solution. *Q Rev Biophys* 40(3):191–285.
50. Pettersen EF, et al. (2004) UCSF Chimera—A visualization system for exploratory research and analysis. *J Comput Chem* 25(13):1605–1612.
51. Chung KM, Diamond MS (2008) Defining the levels of secreted non-structural protein NS1 after West Nile virus infection in cell culture and mice. *J Med Virol* 80(3):547–556.
52. Rumyantsev AA, et al. (2010) Direct random insertion of an influenza virus immunologic determinant into the NS1 glycoprotein of a vaccine Flavivirus. *Virology* 396(2): 329–338.
53. Hall RA, et al. (1999) Loss of dimerisation of the nonstructural protein NS1 of Kunjin virus delays viral replication and reduces virulence in mice, but still allows secretion of NS1. *Virology* 264(1):66–75.
54. Powell AK, Yates EA, Fernig DG, Turnbull JE (2004) Interactions of heparin/heparan sulfate with proteins: Appraisal of structural factors and experimental approaches. *Glycobiology* 14(4):17R–30R.
55. Malpede BM, Lin DH, Tolia NH (2013) Molecular basis for sialic acid-dependent receptor recognition by the *Plasmodium falciparum* invasion protein erythrocyte-binding antigen-140/BAEBL. *J Biol Chem* 288(17):12406–12415.
56. Stahelin RV (2009) Lipid binding domains: More than simple lipid effectors. *J Lipid Res* 50(Suppl):S299–S304.
57. Falconar AK (1997) The dengue virus nonstructural-1 protein (NS1) generates antibodies to common epitopes on human blood clotting, integrin/adhesin proteins and binds to human endothelial cells: Potential implications in haemorrhagic fever pathogenesis. *Arch Virol* 142(5):897–916.
58. Falconar AKI, Martinez F (2011) The NS1 glycoprotein can generate dramatic antibody-enhanced Dengue viral replication in normal out-bred mice resulting in lethal multi-organ disease. *PLoS ONE* 6(6):e21024.
59. Lin Y-S, et al. (2011) Molecular mimicry between virus and host and its implications for Dengue disease pathogenesis. *Exp Biol Med (Maywood)* 236(5):515–523.
60. Sun D-S, et al. (2007) Antiplatelet autoantibodies elicited by Dengue virus nonstructural protein 1 cause thrombocytopenia and mortality in mice. *J Thromb Haemost* 5(11):2291–2299.
61. Studier FW (2005) Protein production by auto-induction in high density shaking cultures. *Protein Expr Purif* 41(1):207–234.
62. Landau M, et al. (2005) ConSurf 2005: The projection of evolutionary conservation scores of residues on protein structures. *Nucleic Acids Res* 33(Web Server issue): W299–W302.